

Unconventional sign-changing superconductivity near quantum criticality in YFe_2Ge_2

Alaska Subedi

Centre de Physique Théorique, École Polytechnique, CNRS, 91128 Palaiseau Cedex, France

(Dated: July 23, 2018)

I present the results of first principles calculations of the electronic structure and magnetic interactions for the recently discovered superconductor YFe_2Ge_2 and use them to identify the nature of superconductivity and quantum criticality in this compound. I find that the Fe 3d derived states near the Fermi level show a rich structure with the presence of both linearly dispersive and heavy bands. The Fermi surface exhibits nesting between hole and electron sheets that manifests as a peak in the susceptibility at $(1/2, 1/2)$. I propose that the superconductivity in this compound is mediated by antiferromagnetic spin fluctuations associated with this peak resulting in a s_{\pm} state similar to the previously discovered iron-based superconductors. I also find that various magnetic orderings are almost degenerate in energy, which indicates that the proximity to quantum criticality is due to competing magnetic interactions.

PACS numbers: 74.20.Mn, 74.40.Kb, 74.25.Jb

Unconventional superconductivity and quantum criticality are two of the most intriguing phenomena observed in physics. The underlying mechanisms and the properties exhibited by the systems in which these two phenomena occur has not been fully elucidated because unconventional superconductors and materials at quantum critical point are so rare. The dearth of realizable examples has also held back the study of the relationship and interplay between unconventional superconductivity and quantum criticality, if there are any.

Therefore, the recent report of non-Fermi liquid behavior and superconductivity in YFe_2Ge_2 by Zou *et al.* is of great interest despite a low superconducting T_c of ~ 1.8 K.¹ This material is also interesting because it shares some important features with the previously discovered iron-based high-temperature superconductors. Like the other iron-based superconductors, its structural motif is a square plane of Fe that is tetrahedrally coordinated, in this case, by Ge. This Fe_2Ge_2 layer is stacked along the z axis with an alternating layer of Y ions. The resulting body-centered tetragonal structure ($I4/mmm$) of this compound is the same as that of the ‘122’ family of the iron-based superconductors.

The nearest neighbor Fe–Ge and Fe–Fe distances of 2.393 and 2.801 Å, respectively, in this compound² are similar to the Fe–As and Fe–Fe distances of 2.403 and 2.802 Å, respectively, found in BaFe_2As_2 .³ This raises the possibility that the direct Fe–Fe hopping is important to the physics of this material, which is the case for the previously discovered iron-based superconductors.⁴

Furthermore, Zou *et al.* report that the superconductivity in this compound exists in the vicinity of a quantum critical point that is possibly associated with antiferromagnetic spin fluctuations.¹ A related isoelectronic compound LuFe_2Ge_2 that occurs in the same crystal structure exhibits antiferromagnetic spin density wave order below 9 K,^{5,6} and the magnetic transition is continuously suppressed in $\text{Lu}_{1-x}\text{Y}_x\text{Fe}_2\text{Ge}_2$ series as Y content is increased, with the quantum critical point lying near the composition $\text{Lu}_{0.81}\text{Y}_{0.19}\text{Fe}_2\text{Ge}_2$.⁷ The proximity of

YFe_2Ge_2 to quantum criticality is observed in the non-Fermi liquid behavior of the specific-heat capacity and resistivity. Zou *et al.* find that the unusually high Sommerfeld coefficient with a value of $C/T \simeq 90$ mJ/mol K² at 2 K further increases to a value of ~ 100 mJ/mol K² as the temperature is lowered, although the experimental data is not detailed enough to distinguish between a logarithmic and a square root increase. They also find that the resistivity shows a behavior $\rho \propto T^{3/2}$ up to a temperature of 10 K.

In this paper, I use the results of first principles calculations to discuss the interplay between superconductivity and quantum criticality in YFe_2Ge_2 in terms of its electronic structure and competing magnetic interactions. I find that the fermiology in this compound is dominated by Fe 3d states with the presence of both heavy and linearly dispersive bands near the Fermi level. The Fermi surface consists of five sheets. There is an open tetragonal electron cylinder around $X = (1/2, 1/2, 0)$. A large three dimensional closed sheet that is shaped like a shell of a clam is situated around $Z = (0, 0, 1/2) = (1, 0, 0)$. This sheet encloses a cylindrical and two almost spherical hole sheets. The tetragonal cylinder sheet around X nests with the spherical and the cylindrical sheets around Z , which manifests as a peak at $(1/2, 1/2)$ in the bare susceptibility. I propose that the superconductivity in this compound is mediated by antiferromagnetic spin fluctuations associated with this peak, and the resulting superconductivity has a sign-changing s_{\pm} symmetry with opposite signs on the nested sheets around X and Z . This superconductivity is similar to the one proposed for previously discovered iron-based superconductors.^{8,9} Furthermore, I find that there are competing magnetic interactions in this compound, and the quantum criticality is due to the fluctuations associated with these magnetic interactions.

The results presented here were obtained within the local density approximation (LDA) using the general full-potential linearized augmented planewave method as implemented in the WIEN2k software package.¹⁰ Muffin-

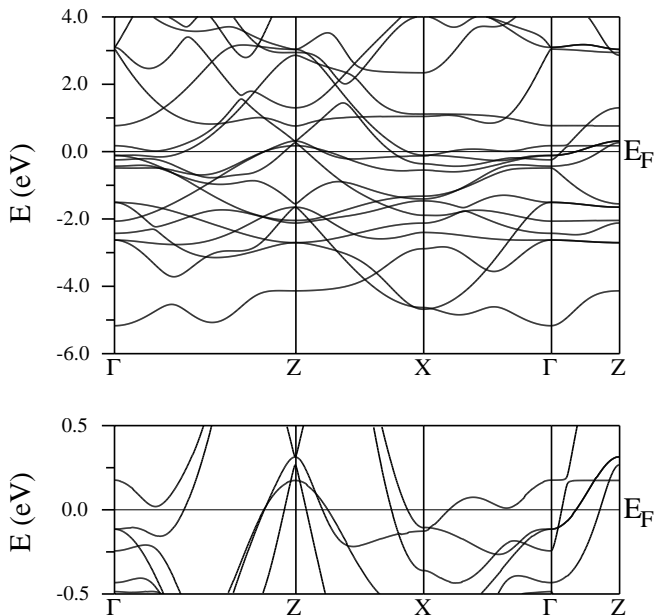


FIG. 1: Top: LDA non-spin-polarized band structure of YFe_2Ge_2 . Bottom: A blow-up of the band structure around Fermi level. The long Γ - Z direction is from $(0, 0, 0)$ to $(1, 0, 0)$ and the short one is from $(0, 0, 0)$ to $(0, 0, 1/2)$. The X point is $(1/2, 1/2, 0)$. The stacking of the Brillouin zone is such that $(1, 0, 0) = (0, 0, 1/2)$. See Fig. 1 of Ref. 13 for a particularly illuminating illustration of the reciprocal-space structure.

tin radii of 2.4, 2.2, and 2.1 a.u. for Y, Fe, and Ge, respectively, were used. A $24 \times 24 \times 24$ k -point grid was used to perform the Brillouin zone integration in the self-consistent calculations. An equivalently sized or larger grid was used for supercell calculations. Some magnetic calculations were also checked with the ELK software package.¹¹ I used the experimental parameters ($a = 3.9617$ and $c = 10.421$ Å),² but employed the internal coordinate for Ge $z_{\text{Ge}} = 0.3661$ obtained via non-spin-polarized energy minimization. The calculated value for z_{Ge} is different from the experimentally determined value of $z_{\text{Ge}} = 0.3789$. The difference in the Ge height between the calculated and experimental structures is 0.13 Å, which is larger than the typical LDA error in predicting the crystal structure. Such a discrepancy is also found in the iron-based superconductors.⁴ This may suggest that YFe_2Ge_2 shares some of the underlying physics with the previously discovered iron-based superconductors.

The non-spin-polarized LDA band structure and density of states (DOS) are shown in Figs. 1 and 2, respectively. The lowest band that starts out from Γ at -5.2 eV relative to the Fermi energy has Ge $4p_z$ character. There is only one band with Ge $4p_z$ character below Fermi level, and there is another band with this character above the Fermi level. This indicates that the Ge ions make covalent bonds along the c axis, which is not surprising given the short Ge-Ge distance in that direction.

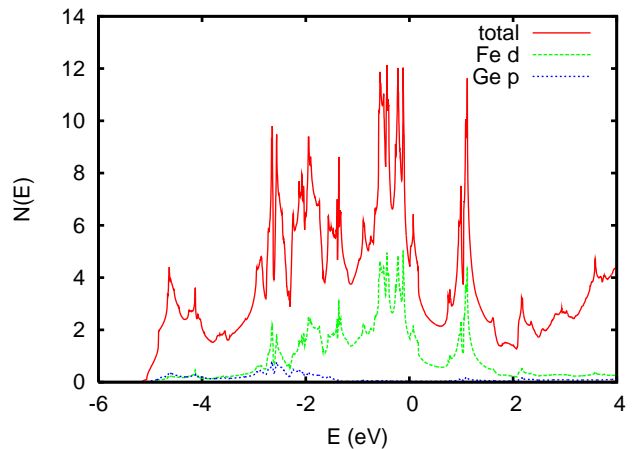


FIG. 2: (Color online) Electronic density of states non-spin-polarized of YFe_2Ge_2 and projections on to the LAPW spheres per formula unit both spin basis.

The four bands between -1.2 and -4.8 eV that start out from Γ at -1.5 and -2.6 eV have Ge $4p_x$ and $4p_y$ character. Rest of the bands below the Fermi level have mostly Fe $3d$ character. Similar to the other iron-based superconductors,⁴ there is no gap-like structure among the Fe $3d$ bands splitting them into a lower lying e_g and higher lying t_{2g} states. This shows that Fe-Ge covalency is minimal and direct Fe-Fe interactions dominate. Almost all of the Fe $4s$ and Y $4d$ and $5s$ character lie above the Fermi level. This indicates a nominal occupation of Fe $3d^{6.5}$, although the actual occupancy will be different because there is some covalency of Fe $3d$ states with Y $4d$ and Ge $4p$ states.

The electronic states near the Fermi level come from Fe $3d$ derived bands and show a rich structure. The electronic DOS at the Fermi level is $N(E_F) = 4.50$ eV⁻¹ on a per formula unit both spin basis corresponding to a calculated Sommerfeld coefficient of 10.63 mJ/mol K². The Fermi level lies at the bottom of a valley with a large peak due to bands of mostly d_{xz} and d_{yz} characters on the left and a small peak due to a band of mostly d_{xy} character on the right. (The local coordinate system of the Fe site is rotated by 45° in the xy plane with respect to the global cartesian axes such that the Fe $d_{x^2-y^2}$ orbital points away from the Ge p_x and p_y orbitals.) There is a pair of linearly dispersive band with mostly d_{xz} and d_{yz} as well as noticeable Ge p_z characters either side of Z . If they are not gapped in the superconducting state, they will provide the system with a massless excitation. In addition to this pair of linearly dispersive bands, there is also a very flat band near the Fermi level along X - Γ . This band has an electron-like nature around X and crosses the Fermi level close to it. Along the X - Γ direction, it reaches a maximum at 0.08 eV above the Fermi level, turns back down coming within 0.01 eV of touching the Fermi level, and again moves away from the Fermi level. It may be possible to access these band critical points

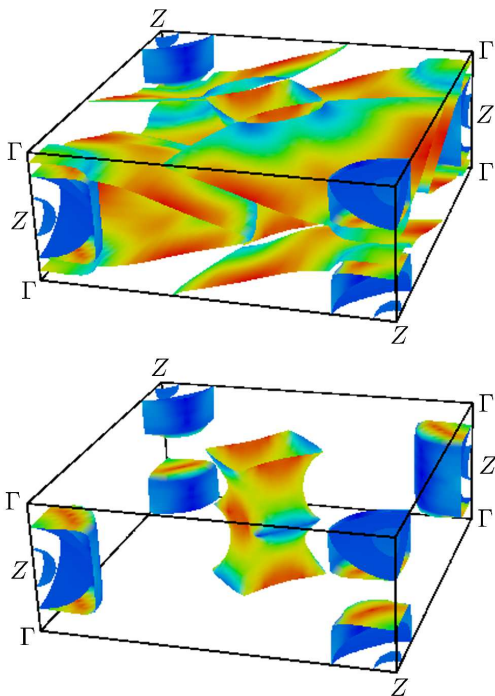


FIG. 3: (Color online) Top: LDA Fermi surface of YFe_2Ge_2 . Bottom: The Fermi surface without the large sheet. The shading is by velocity.

that have vanishing quasiparticle velocities via small perturbations due to impurities, doping, or changes in structural parameters. The role of such band critical points in quantum criticality has been emphasized recently,¹² and similar physics may be relevant in this system.

The Fermi surface of this compound is shown in Fig. 3. There is an open very two dimensional tetragonal electron cylinder around X . This has mostly d_{xz} and d_{yz} character. There are four closed sheets around Z . One of them is a large three dimensional sheet with the shape like the shell of a clam with d_{xz} , d_{yz} , d_{xy} , and d_{z^2} characters. There are two almost spherical hole sheets. These have mostly d_{xz} and d_{yz} characters, with the smaller one also containing noticeable Ge p_z character. These two spherical sheets are enclosed by a closed cylindrical hole sheet that has mostly d_{xy} character.

The cylindrical and larger spherical sheets centered around Z touch at isolated points. Otherwise, the Fermi surface is comprised of disconnected sheets. If one considers the Γ - Z - Γ path along the k_z direction, there is a series of box-shaped cylindrical hole sheet that encloses the two spherical sheets. Although there are no sections around Γ , these sheets around Z enclose almost two-third of the Γ - Z - Γ path. Therefore, there is likely to be substantial nesting between the sheets around Z and X that will lead to a peak in the susceptibility at the wave vector $(1/2, 1/2)$.

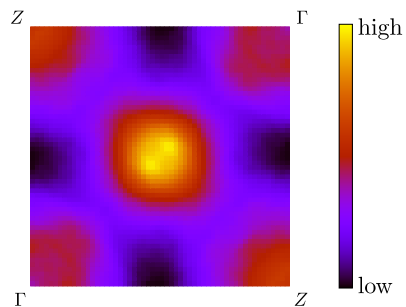


FIG. 4: The real part of bare susceptibility calculated with the matrix element set to unity.

I have calculated the Lindhard susceptibility

$$\chi_0(q, \omega) = \sum_{k,m,n} |M_{k,k+q}^{m,n}|^2 \frac{f(\epsilon_k^m) - f(\epsilon_{k+q}^n)}{\epsilon_k^m - \epsilon_{k+q}^n - \omega - i\delta}$$

at $\omega \rightarrow 0$ and $\delta \rightarrow 0$, where ϵ_k^m is the energy of a band m at wave vector k and f is the Fermi distribution function. M is the matrix element, which is set to unity. The real part of the susceptibility is shown in Fig. 4, and it shows peaks at Γ , Z , and X with the peak at X having the highest magnitude. Note, however, that the cylinders around Z and X have different characters, which should reduce the peak X and make it broader as well. The peak at Γ is equal to the DOS $N(E_F)$. The peak at Z reflect the nesting along the flat sections of the sheets along $(0, 0, 1/2)$ direction, while the peak at X is due to the nesting between the hole cylinder and spheres centered around Z and the electron cylinder centered around X .

The bare Lindhard susceptibility is further enhanced due to the RPA interaction, and its real part is related to magnetism and superconductivity. It is found experimentally that pure YFe_2Ge_2 does not order magnetically down to a temperature of 2 K although it shows non-Fermi liquid behavior in the transport and heat capacity measurements that is likely due to proximity to a magnetic quantum critical point.¹ As the temperature is lowered further, superconductivity manifests in the resistivity measurements at $T_c^p = 1.8$ K and DC magnetization at $T_c^{\text{mag}} = 1.5$ K. This superconductivity can be due spin fluctuations associated with the peak in the susceptibility.^{14,15} The pairing interaction has the form

$$V(q = k - k') = -\frac{I^2(q)\chi_0(q)}{1 - I^2(q)\chi_0^2(q)}$$

in the singlet channel and is repulsive. (In the triplet channel, the interaction is attractive and also includes an angular factor.) Here $I(q)$ is the Stoner parameter which microscopically derives from Coulomb repulsion between electrons.

In the present case, the structure of the calculated susceptibility leads to the off-diagonal component of the interaction matrix to have a large negative value $-\lambda$ for the pairing between the hole sheets at Z and electron cylinder

at X in the singlet channel. The diagonal component of the interaction matrix λ_d pairing interactions on the hole and electron sheets are small and ferromagnetic. (For simplicity, I have assumed that the density of states are same for the hole and electron sections.) The eigenvector corresponding to the largest eigenvalue of this interaction matrix has opposite signs between the hole sheets around Z and electron cylinder around X , and this is consistent with a singlet s_{\pm} superconductivity with a wave vector $(1/2, 1/2)$. This superconductivity is similar to the previously discovered iron-based superconductors.^{8,9}

The proposed superconductivity in YFe_2Ge_2 and the previously discovered iron-based superconductor is similar, but the $T_c = 1.8$ K for YFe_2Ge_2 is much smaller than those reported for other iron-based superconductors. One reason for this may be the smaller nesting in this compound leading to a smaller peak in susceptibility. The hole cylinder around Z has mostly d_{xy} character whereas the hole spheres around Z and the electron cylinder around X have mostly d_{xz} and d_{yz} character. These factors should lead to a slightly smaller and broader peak at X . I note, however, that nesting in the other iron-based superconductors is also not perfect⁸ and the band characters between the nested sheets also vary.⁹

Another reason for the smaller T_c in YFe_2Ge_2 may be due to the existence of competing magnetic fluctuations associated with the proximity to quantum criticality. The DOS from non-spin-polarized calculation is $N(E_F) = 1.125$ eV⁻¹ per spin per Fe, which puts this material on the verge of a ferromagnetic instability according to the Stoner criterion. Ferromagnetism is pair-breaking for the singlet pairing and will suppress the T_c in this compound. Furthermore, there is a peak in the susceptibility at Z as well. The presence of additional antiferromagnetic interactions might reduce the phase space available for the spin fluctuation associated with the pairing channel and may be pair-breaking as well.

TABLE I: The relative energies of various magnetic orderings and the moments within the Fe spheres. These are almost degenerate, indicating the proximity to quantum criticality is due to competing magnetic interactions.

	Energy (meV/Fe)	Moment (μ_B /Fe)
NSP	0	0
FM	-6.29	0.59
AFM (0,0,1/2)	-11.63	0.64
SDW (1/2,1/2,0)	-6.52	0.72

I performed magnetic calculations with various orderings on $(1 \times 1 \times 2)$ and $(\sqrt{2} \times \sqrt{2} \times 2)$ supercells to check the strength of competing magnetic interactions. The relative energies and the Fe moments are summarized in Table I. I was able to stabilize various magnetic configurations, and their energies are close to that of the non-spin-polarized configuration. However, I was not able to stabilize the checkerboard antiferromagnetic order in the ab plane. When the magnetic order is stabilized, the

magnitude of the Fe moment is less than $1 \mu_B$, and the magnitudes vary between different orderings. This indicates that the magnetism is of itinerant nature. It is worthwhile to note that LDA calculations overestimate the magnetism in this compound as it does not exhibit any magnetic order experimentally. This disagreement between LDA and experiment is different from that for the Mott insulating compounds where LDA in general underestimates the magnetism.

Although this compound does not magnetically order experimentally, it nonetheless shows proximity to magnetism. It is found that partial substitution of Y by isovalent Lu causes the system to order antiferromagnetically, with 81% Lu substitution being the critical composition.⁷ At substitution values below the critical composition, the system shows non-Fermi liquid behavior in the heat capacity and transport measurements.¹ The unusually high Sommerfeld coefficient of ~ 90 mJ/mol K² at 2 K further increases as the temperature is lowered and the resistivity varies as $\rho \propto T^{3/2}$ up to around 10 K. This non-Fermi liquid behavior and the large renormalization of the magnetic moments may happen because there is a large phase for competing magnetic tendencies in this compound. This is due to the fluctuation-dissipation theorem, which relates the fluctuation of the moment to the energy and momentum integrated imaginary part of the susceptibility.¹⁶⁻²⁰ If the quantum criticality is due to competing magnetic interactions, the inelastic neutron scattering experiments, which measures the imaginary part of the susceptibility, would exhibit the structure related to the competing interactions. Therefore, even though this compound does not show magnetic ordering, it would be useful to perform such experiments and compare with the results presented here.

In any case, I indeed find that various magnetic orderings and the non-spin-polarized configuration are close in energy (see Table I). The energy of the lowest magnetic configuration is only 11.6 meV/Fe lower than the non-spin-polarized one, and the energies of the different magnetic orderings are within 6 meV/Fe of each other. As a comparison, the difference in energy between the non-magnetic configuration and the most stable magnetic ordering in BaFe_2As_2 is 92 meV/Fe, and the energy of the magnetic ordering closest to the most stable one is higher by 51 meV.²¹ Signatures of quantum criticality has been reported for BaFe_2As_2 and related compounds.²²⁻²⁴ YFe_2Ge_2 should show pronounced effects of proximity to quantum criticality as the competition between magnetic interactions is even stronger.

In summary, I have discussed the superconductivity and quantum criticality in YFe_2Ge_2 in terms of its electronic structure and competing magnetic interactions. The electronic states near the Fermi level are derived from Fe 3d bands and show a rich structure with the presence of both linearly dispersive and heavy bands. The Fermi surface consists of five sheets. There is an open rectangular electron cylinder around X . A big sheet shaped like the shell of a clam encloses a hole cylinder and

two hole spheres around Z . There is a peak in the bare susceptibility at $(1/2, 1/2)$ due to nesting between the hole sheets around Z and the electron cylinder around X . I propose that the superconductivity in YFe_2Ge_2 is due to antiferromagnetic spin fluctuations associated with this peak. The resulting superconducting state has a s_{\pm} state similar to that of previously discovered iron-based superconductors. I also find that different magnetic configura-

tions are close in energy, which suggests the presence of competing magnetic interactions that are responsible for the proximity to quantum criticality observed in this compound.

I am grateful to Antoine Georges for helpful comments and suggestions. This work was partially supported by a grant from Agence Nationale de la Recherche (PNICTIDES).

-
- ¹ Y. Zou, Z. Feng, P. W. Logg, J. Chen, G. I. Lampronti, and F. M. Grosche, arXiv e-print, 1311:0247.
- ² G. Venturini, and B. Malaman, *J. Alloys Compounds* **235**, 201 (1996).
- ³ M. Rotter, M. Tegel, D. Johrendt, I. Schellenberg, W. Hermes, and R. Pöttgen, *Phys. Rev. B* **78**, 020503(R) (2008).
- ⁴ D. J. Singh, and M.-H. Du, *Phys. Rev. Lett.* **100**, 237003 (2008).
- ⁵ M. Avila, S. Bud'ko, and P. Canfield, *J. Magn. Magn. Mater.* **270**, 51 (2004).
- ⁶ J. Ferstl, H. Rosner, and C. Geibel, *Physica B: Condens. Matter* **378-380**, 744 (2006).
- ⁷ S. Ran, S. L. Bud'ko, and P. C. Canfield, *Philosophical Magazine* **91**, 4388 (2011).
- ⁸ I. I. Mazin, D. J. Singh, M. D. Johannes, and M. H. Du, *Phys. Rev. Lett.* **101**, 057003 (2008).
- ⁹ K. Kuroki, S. Onari, R. Arita, H. Usui, Y. Tanaka, H. Kotani, H. Aoki, *Phys. Rev. Lett.* **101**, 087004 (2008).
- ¹⁰ P. Blaha, K. Schwarz, G. Madsen, D. Kvasnicka, and J. Luitz, "WIEN2k, An Augmented Plane Wave + Local Orbitals Program for Calculating Crystal Properties" (K. Schwarz, Tech. Univ. Wien, Austria) (2001).
- ¹¹ <http://elk.sourceforge.net>.
- ¹² B. P. Neal, E. R. Ylvisaker, and W. E. Pickett, *Phys. Rev. B* **84**, 085133 (2011).
- ¹³ J. T. Park, D. S. Inosov, A. Yaresko, S. Graser, *et al.*, *Phys. Rev. B* **82**, 134503 (2010).
- ¹⁴ N. F. Berk and J. R. Schrieffer, *Phys. Rev. Lett.* **17**, 433 (1966).
- ¹⁵ D. Fay and J. Appel, *Phys. Rev. B* **22**, 3173 (1970).
- ¹⁶ T. Moriya, *Spin Fluctuations in Itinerant Electron Magnetism* (Springer, Berlin, 1985).
- ¹⁷ A. Z. Solontsov and D. Wagner, *Phys. Rev. B* **51**, 12410 (1995).
- ¹⁸ A. Ishigaki and T. Moriya, *J. Phys. Soc. Jpn.* **67**, 3924 (1998).
- ¹⁹ A. Aguayo, I. I. Mazin, and D. J. Singh, *Phys. Rev. Lett.* **92**, 147201 (2004).
- ²⁰ P. Larson, I. I. Mazin, and D. J. Singh, *Phys. Rev. B* **69**, 064429 (2004).
- ²¹ D. J. Singh, *Phys. Rev. B* **78**, 094511 (2008).
- ²² F. Ning, K. Ahilan, T. Imai, A. S. Sefat, R. Jin, M. A. McGuire, B. C. Sales, D. Mandrus, *J. Phys. Soc. Jpn.* **78**, 013711 (2009).
- ²³ S. Jiang, H. Xing, G. Xuan, C. Wang, Z. Ren, C. Feng, J. Dai, Z. Xu, G. Cao, *J. Phys. Condens. Matter* **21**, 382203 (2009).
- ²⁴ S. Kasahara, T. Shibauchi, K. Hashimoto, K. Ikada, S. Tonegawa, R. Okazaki, H. Shishido, H. Ikeda, H. Takeya, K. Hirata, T. Terashima, Y. Matsuda, *Phys. Rev. B* **81**, 184519 (2010).